

Exciton quasicondensation in one-dimensional systems

Yochai Werman and Erez Berg

Weizmann Institute of Science, Rehovot, Israel

(Received 13 August 2014; revised manuscript received 22 April 2015; published 10 June 2015)

Two Luttinger liquids, with an equal density and opposite sign of charge carriers, may exhibit enhanced excitonic correlations. We term such a system an exciton quasicondensate, with a possible realization being two parallel oppositely doped quantum wires, coupled by repulsive Coulomb interactions. We show that this quasiexciton condensate can be stabilized in an extended range of parameters, in both spinless and spinful systems. We calculate the interwire tunneling current-voltage characteristic, and find that a negative differential conductance is a signature of excitonic correlations. For spinful electrons, the excitonic regime is shown to be distinct from the usual quasi-long-range ordered Wigner crystal phase characterized by power-law density wave correlations. The two phases can be clearly distinguished through their interwire tunneling current-voltage characteristics. In the quasiexciton condensate regime the tunneling conductivity diverges at low temperatures and voltages, whereas in the Wigner crystal it is strongly suppressed. Both the Wigner crystal and the excitonic regime are characterized by a divergent Coulomb drag at low temperature. Finally, metallic carbon nanotubes are considered as a special case of such a one-dimensional setup, and it is shown that exciton condensation is favorable due to the additional valley degree of freedom.

DOI: [10.1103/PhysRevB.91.245410](https://doi.org/10.1103/PhysRevB.91.245410)

PACS number(s): 73.21.-b, 71.35.-y, 81.07.Vb, 73.22.-f

I. INTRODUCTION

Excitons are bound states between an electron and a positively charged hole. Similar to Cooper pairs, which are bound states of two electrons, excitons are bosons, and may form a condensate. The exciton condensate phase has been studied extensively, both theoretically and experimentally, and in the last few years several groups have reported physical signatures of such a phase in two-dimensional bilayers coupled by Coulomb interactions [1–4]. Two typical experiments are performed in order to probe exciton condensation—counterflow Coulomb drag [3–5], in which the current flow through only one of the layers is suppressed due to interlayer scattering, and tunneling [6], whereby the current between the layers is enhanced at low voltages.

Although long-range excitonic order cannot exist in one dimension (1D), an exciton quasicondensate (corresponding to enhanced exciton correlations that decay as a power law as a function of distance) can occur at zero temperature. Such a quasicondensate has signatures in both tunneling and Coulomb drag experiments. In this paper, we consider a system of two parallel quantum wires with an opposite sign of the carriers. We calculate the interwire tunneling current-voltage characteristics in different regimes. We show that the exciton correlations manifest themselves in an enhancement of the interwire current at low voltages. In particular, a negative differential conductance is a signature of exciton quasicondensation. In addition, we consider the special case of a pair of oppositely gated parallel carbon nanotubes, for which we show that exciton quasicondensation is particularly favorable [7].

For simplicity, we begin with a spinless model (Sec. II). The addition of spin in Sec. III introduces an incompatibility between tunneling and interwire backscattering, resulting in modified I - V curves corresponding to the case of either tunneling or backscattering dominated systems. To conclude, we consider the case of carbon nanotubes (Sec. IV), which are a natural experimental realization of our model, and

display an additional electronic degree of freedom—the valley.

II. SPINLESS FERMIONS

A. Model

We commence our analysis with spinless fermions. The theoretical system under consideration is composed of two parallel, infinitely long one-dimensional wires, one of which is doped with electrons and the other with holes (see Figs. 1 and 2). The density of carriers in the two wires is identical, so that the Fermi momenta are equal, $k_{F1} = k_{F2}$. The system is described by the Hamiltonian

$$H = H_{\text{kin}} + H_{\text{int}}. \quad (1)$$

Here, $H_{\text{kin}} = -i \sum_{j,\eta} v_F \int dx c_{j\eta}^\dagger (j\eta \partial_x) c_{j\eta}$, where $c_{j\eta}^\dagger$ is the creation operator for a right/left moving ($\eta = \pm 1$) electron in wire $j = \pm 1$; the spectrum has been linearized around k_F . H_{int} is the interaction Hamiltonian, to be specified below. At this stage, we neglect the interwire tunneling. A system of two wires coupled by four-fermion interactions (but not by single-electron tunneling) has been studied by various authors (see, e.g., Refs. [8–10]); the different element in the present discussion is the fact that the charges in the two wires are of opposite sign.

It is helpful to revert to the bosonized representation of one-dimensional electrons [11], where $c_{i\eta}^\dagger \sim e^{i(\eta\phi_i - \theta_i)}$. The bosonic field ϕ_i is related to the electronic charge density fluctuations by $\sum_\eta c_{i\eta}^\dagger c_{i\eta} = \partial_x \phi_i / \pi$. θ_i is similarly related to the electronic current fluctuations. In terms of the bosonic variables, the small momentum (forward scattering) part of the interaction becomes quadratic. The Hamiltonian takes the form $H = H_0 + H_1$, where the quadratic part of the Hamiltonian results in the Tomonaga-Luttinger form

$$H_0 = \sum_{\lambda=\pm} \frac{u_\lambda}{2\pi} \int dx \left[K_\lambda (\partial_x \theta_\lambda)^2 + \frac{1}{K_\lambda} (\partial_x \phi_\lambda)^2 \right], \quad (2)$$

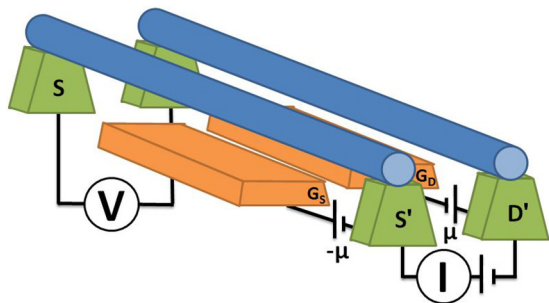


FIG. 1. (Color online) Proposed setup of the system. The two wires (in this figure, carbon nanotubes) are suspended via the green metallic contacts above additional gates. The voltage difference between the contacts and the gates controls the doping of the nanotubes, and we choose this voltage to be opposite for the two wires (μ and $-\mu$ in the figure) so that CNT S is electron doped and CNT D hole doped, with the same density of charge carriers. In a tunneling experiment, a voltage difference is placed between contacts S' and D' , forcing a tunneling current between the two nanotubes, which is measured. The resulting voltage difference between the two nanotubes may be read off the voltmeter placed between D and S , which gives $V + 2\mu$, V being the desired quantity.

where we have introduced the fields $\phi_{\pm} = \frac{1}{\sqrt{2}}(\phi_1 \pm \phi_{-1})$, and similarly θ_{\pm} . u_{\pm} are the velocities of the plasmons, and K_{\pm} are the corresponding Luttinger parameters, given by $K_{\pm} = \frac{K}{\sqrt{1 \pm UK}}$, where K is the Luttinger parameter of an individual wire (including the effect of the intrawire interactions). $U = V_{q=0}/2v_F$ is the dimensionless interwire forward scattering strength between electrons (V_q is the Fourier transform of

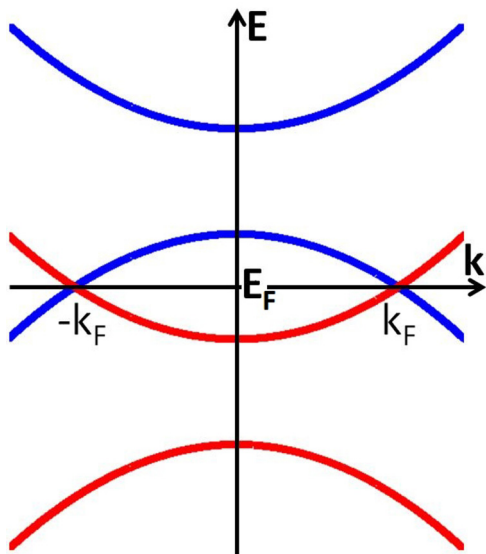


FIG. 2. (Color online) The dispersion relation for the two wires. The upper, red dispersion represents the electron-doped wire, while the other is hole doped. The densities of charge carriers are the same for both wires, and therefore k_F is identical. Tunneling between the two wires connects right movers from one wire to left movers from the other. The spectrum is linearized around each Fermi point, and the slopes, equal to the Fermi velocity v_F , are assumed to be of the same magnitude for simplicity.

the interwire density-density interaction). We consider $U > 0$, corresponding to a repulsive (Coulomb) interwire interaction.

In addition to the forward scattering term, which is quadratic in the bosonic fields, backscattering between the wires is also possible, and gives rise to the term

$$\begin{aligned} H_{BS} &= V_{q=2k_F} \int dx c_{1R}^{\dagger} c_{1L} c_{-1R}^{\dagger} c_{-1L} + \text{H.c.} \\ &= -|V_{BS}| \int dx \cos(2\sqrt{2}\phi_{+}), \end{aligned} \quad (3)$$

where $V_{BS} \propto V_{q=2k_F}$ is the strength of the backscattering interactions. Note the minus sign in Eq. (3), which arises from the commutation relations between the ϕ and θ fields (see Appendix A). If only small momentum scattering is present ($V_{BS} = 0$), the two modes are massless, and the correlations of physical observables decay as power laws for any interaction strength. The operators with the most slowly decaying correlations are the $2k_F$ component of the density, giving rise to the density-density correlation function decaying as $\langle c_{j,R}^{\dagger}(x)c_{j,L}(x)c_{j,L}^{\dagger}(0)c_{j,R}(0) \rangle \sim 1/x^{K_+ + K_-}$, and exciton (particle-hole pair) correlations, which satisfy $\langle c_{1,R}^{\dagger}(x)c_{-1,L}(x)c_{-1,L}^{\dagger}(0)c_{1,R}(0) \rangle \sim 1/x^{K_+ + 1/K_-}$. Order parameters similar to the exciton order parameter studied here have been studied previously (see, for example, Ref. [11], Chap. 8), but the fact that the wires are oppositely doped in this system allows for qualitatively different features. In particular, in this case interwire tunneling is enhanced at low energies, as we discuss below.

In the presence of backscattering ($V_{BS} \neq 0$), and if backscattering is relevant (which is the case for $K_+ < 1$), a gap $\Delta_{BS} \propto V_{BS}^{1/(2-2K_+)}$ opens in the spectrum of total charge fluctuations. The partially gapped phase has enhanced Wigner crystalline (density-density) correlations. As we will show, in the spinless case this phase also displays enhanced excitonic correlations.

B. Interwire tunneling

Tunneling current measurements are a sensitive experimental method by which to probe exciton correlations. Tunneling from an external lead into an interacting one-dimensional system is normally suppressed [12–15]; this is a result of the strong correlations between electrons in a Luttinger liquid, which resist the entrance of an external, uncorrelated particle. In our system of two coupled wires, on the other hand, exciton correlations between the two wires tend to enhance the tunneling current, since particles in one wire are aligned with holes in the other.

In an experiment by Spielman *et al.* [6], signatures of exciton condensation have been detected in a two-dimensional bilayer subject to a high magnetic field. A sharp peak in the differential interlayer tunneling conductivity $\sigma(V) = \frac{dI}{dV}$ (where I_t is the tunneling current density and V the interlayer voltage) at zero bias has been interpreted as a signature of such long-range order [16]. Here, we present theoretical predictions regarding the tunneling current-voltage relations in the one-dimensional equivalent of the system studied in Ref. [6].

In order to allow for a tunneling current, weak interwire hopping is added to the Hamiltonian,

$$\begin{aligned} H_{\text{tun}} &= -\tilde{t}_{\perp} \sum_{i\eta} \int dx c_{i\eta}^{\dagger}(x) c_{-i-\eta}(x) \\ &= -t_{\perp} \int dx \cos(\sqrt{2}\phi_{+}) \sin(\sqrt{2}\theta_{-}), \end{aligned} \quad (4)$$

where \tilde{t}_{\perp} is the interwire tunneling amplitude, and $t_{\perp} \propto \tilde{t}_{\perp}$ [the proportionality constant being $1/(2\pi a)$ in a naive continuum limit, where a is the short distance cutoff]. The renormalization group (RG) equations for the two nonquadratic terms, the interwire backscattering (3) and tunneling, are

$$\begin{aligned} \frac{dV_{\text{BS}}}{ds} &= [2 - 2K_{+}] V_{\text{BS}}, \\ \frac{dt_{\perp}}{ds} &= \left[2 - \frac{1}{2} \left(K_{+} + \frac{1}{K_{-}} \right) \right] t_{\perp}. \end{aligned} \quad (5)$$

Here, s is the momentum scaling parameter, $\Lambda(s) = \Lambda_0 e^{-s}$. We work in the limit where both the bare backscattering and tunneling are very weak.

Tunneling is relevant for $K_{+} + K_{-}^{-1} < 4$, which corresponds to a wide range of physical parameters. In this regime, a gap $\Delta_t \propto t_{\perp}^{1/[2-\frac{1}{2}(K_{+}+K_{-}^{-1})]}$ is opened for fluctuations of the total density and relative charge. In addition, when backscattering is relevant, which is the case for $K_{+} < 1$, the fluctuations of the total density are further suppressed, renormalizing the corresponding Luttinger parameter to zero. We assume that the backscattering gap is larger than the tunneling energy scale in the rest of the section.

C. Current-voltage characteristics

A linear response calculation for the current is applicable when tunneling is irrelevant, or when the voltage is much larger than the tunneling gap. The tunneling current is then approximated by [17]

$$I_t(V) = 2|t_{\perp}|^2 \text{Im} \left\{ G_A^{\text{ret}}(q=0, \omega = -eV) \right\}, \quad (6)$$

where $G_A^{\text{ret}}(q, t) = -i\Theta(t) \langle [A(q, t), A^{\dagger}(-q, 0)] \rangle$ and $A(x, t) = c_1^{\dagger}(x, t) c_{-1}(x, t)$. The linear response calculations result in power laws in the voltage, with the exponents governed by the Luttinger parameters, corresponding to the fact that current dissipates through the excitation of plasmons in the Luttinger liquid. The exponents distinguish between regimes where different sectors are locked; for $\Delta_{\text{BS}} \ll eV$, we get $I_t \sim V^{K_{+}+1/K_{-}-2}$, while for $\Delta_t \ll eV \ll \Delta_{\text{BS}}$ fluctuations in the total density are suppressed, and $I_t \sim V^{1/K_{-}-2}$. If the tunneling operator is irrelevant below Δ_{BS} (as is the case for $K_{-} < 1/4$, corresponding to intrawire interactions much stronger than the interwire ones), this power-law behavior extends all the way to $V = 0$. At small voltages, the current is suppressed because of the strong intrawire correlations. A similar effect was discussed in two-dimensional systems in a perpendicular magnetic field (see Johansson [18]).

When tunneling is relevant, at high enough temperatures such that $T \gtrsim eV$, the linear response still holds. In this case, the low voltage behavior is Ohmic, $I \propto f(T)V$, where $f(T) =$

$T^{-(3-K_{+}-1/K_{-})}$; the finite temperature retarded Green's function that appears in Eq. (6) is given by [11]

$$G_A^{\text{ret}}(q=0, \omega) \propto T^{\alpha-2} B \left(-i \frac{\omega}{4\pi T} + \frac{\alpha}{4}, 1 - \frac{\alpha}{2} \right)^2, \quad (7)$$

with $\alpha = K_{+} + 1/K_{-}$, and B is defined as

$$B(x, y) = \frac{\Gamma(x)\Gamma(y)}{\Gamma(x+y)}. \quad (8)$$

Expanding to first order in ω gives an imaginary part proportional to $T^{\alpha-3}\omega$. Inserting into Eq. (6) results in an Ohmic behavior for low voltages, as described above.

If tunneling is relevant, the $T = 0$ low voltage behavior ($eV \ll \Delta_t$) is dramatically different. The linear response approximation breaks down, as can be seen from the fact that the perturbative expression for the current diverges in the limit $V \rightarrow 0$. At the same time, higher-order terms in the series expansion of the current become increasingly large. In this case, the relative phase field θ_{-} is locked, signifying that charge may fluctuate freely between the two wires, without exciting plasmons. In order to analyze this case, we use a generalization of the ‘‘tilted washboard’’ model for Josephson junctions [19]. Imagine driving a small current density \mathcal{J} between the two wires. The system is described by following effective Hamiltonian,

$$H_{\text{eff}} = H_0 - \int dx \left[J \sin(\sqrt{2}\theta_{-}) - \frac{\sqrt{2}}{e} \mathcal{J} \theta_{-} \right], \quad (9)$$

where $J = t_{\perp} \langle \cos(\sqrt{2}\phi_{+}) \rangle$. (We assume that the field ϕ_{+} is pinned to zero by H_{BS} .) According to the Josephson relation, the interwire current density operator is given by $\sqrt{2}eJ \cos(\sqrt{2}\theta_{-})$, and the voltage is given by $(\sqrt{2}/e)d\theta_{-}/dt$. Dissipation occurs by the creation of soliton-antisoliton pairs that dissociate and induce phase slips of 2π in $\sqrt{2}\theta_{-}$. The voltage is given by

$$V = \frac{2\pi}{e} \Gamma, \quad (10)$$

with Γ the dissociation rate. These propagating soliton-antisoliton pairs correspond to macroscopic quantum tunneling between consecutive minima of the sine-Gordon potential $\sin(\sqrt{2}\theta_{-})$, whose degeneracy is broken by the tunneling current. We have calculated the rate of macroscopic quantum tunneling using the instanton method (see Appendix B for the details of the calculation). The result is $\Gamma \propto e^{-\frac{\alpha}{\mathcal{J}}}$, with $\alpha \approx 2.5e\sqrt{\frac{u-K}{2\pi}}J$. This leads to the highly singular current-voltage relationship

$$I_t(V) \propto -\frac{1}{\log(V)}. \quad (11)$$

Here I_t is the tunneling current and V the interwire voltage.

Our results for spinless electrons are summarized in Table I, and a typical I - V curve is displayed in Fig. 3.

The negative differential conductance, which may extend even above Δ_{BS} , is a clear signature of exciton condensation. This is because no such negative slope will be found in decoupled wires, where the exponent will be $\alpha = 1/K + K - 2 > 0$.

TABLE I. The tunneling current dependence on interwire voltage V for spinless fermions. When $K_+ + 1/K_- < 4$, tunneling is relevant. For voltages below the tunneling gap Δ_t , the tunneling I - V relationship is a singular function, resulting in a diverging tunneling resistivity. For voltages above the gap, and when tunneling is irrelevant, the I - V curves obey power laws, as expected in one-dimensional systems, with the exponents distinguishing between the regime in which the total density is locked by the relevant backscattering process to that in which it is free. The high temperature system displays Ohmic behavior at low voltages.

	$T = 0$			$T \gg \Delta_t, \Delta_{BS}$	
	$\Delta_t \gg V$	$\Delta_{BS} \gg V \gg \Delta_t$	$V \gg \Delta_{BS}$	$V \ll T$	$V \gg T$
Tunneling relevant	$I(V) \propto \frac{-1}{\log(V)}$	$I(V) \propto V^{1/K_- - 2}$	$I(V) \propto V^{K_+ + 1/K_- - 2}$	$I(V) \propto f(T)V$	$I(V) \propto V^{K_+ + 1/K_- - 2}$
Tunn. irrelevant	$I(V) \propto V^{1/K_- - 2} (\Delta_t = 0)$		$I(V) \propto V^{K_+ + 1/K_- - 2}$		

III. SPINFUL ELECTRONS

We now consider the case of spinful electrons. The quadratic part of the Hamiltonian is

$$H_0 = \sum_{\mu, \lambda = \pm} \frac{u_{\mu\lambda}}{2\pi} \int dx \left[K_{\mu\lambda} (\partial_x \theta_{\mu\lambda})^2 + \frac{1}{K_{\mu\lambda}} (\partial_x \phi_{\mu\lambda})^2 \right], \quad (12)$$

where, following standard notation, $\phi_{\mu\pm} = \frac{1}{\sqrt{2}}(\phi_{1\mu} \pm \phi_{2\mu})$, $\mu = \rho, \sigma$, where $\phi_{i, \rho/\sigma} = \frac{1}{\sqrt{2}}(\phi_{i\uparrow} \pm \phi_{i\downarrow})$. $\theta_{\rho, \pm}, \theta_{\sigma, \pm}$ are defined in a similar fashion. $u_{\sigma\pm}, u_{\rho\pm}$ are the velocities of the spin and charge plasmons, and $K_{\sigma\pm}, K_{\rho\pm}$ are the corresponding Luttinger parameters. Assuming that there are only density-density interwire interactions, spin rotation invariance requires $K_{\sigma\pm} = 1$. The charge Luttinger parameters are $K_{\rho\pm} = \frac{K_\rho}{\sqrt{1 \pm UK_\rho}}$, where K_ρ is the charge Luttinger parameter of an individual wire.

In the spinful model, the $2k_F$ interwire backscattering is adverse to exciton quasicondensation; it takes the

form

$$H_{BS} = -|V_{BS}| \int dx \cos(2\phi_{\rho+}) [\cos(2\phi_{\sigma+}) + \cos(2\phi_{\sigma-})], \quad (13)$$

while the tunneling of spinful electrons is described by (see Appendix A)

$$H_{\text{tun}} = t_\perp \int dx [\cos(\phi_{\rho+}) \cos(\phi_{\sigma+}) \cos(\theta_{\sigma-}) \sin(\theta_{\rho-}) - \sin(\phi_{\rho+}) \sin(\phi_{\sigma+}) \sin(\theta_{\sigma-}) \cos(\theta_{\rho-})]. \quad (14)$$

It can be seen that the backscattering term tends to lock the field $\phi_{\sigma-}$ (that describes relative spin fluctuations), and therefore it suppresses the transfer of electrons between the wires. Thus the tunneling and backscattering terms compete with each other in this case. The scaling equations for these two terms are

$$\begin{aligned} \frac{dV_{BS}}{ds} &= [1 - K_{\rho+}] V_{BS}, \\ \frac{dt_\perp}{ds} &= \left[\frac{3}{2} - \frac{1}{4} \left(K_{\rho+} + \frac{1}{K_{\rho-}} \right) \right] t_\perp. \end{aligned} \quad (15)$$

The spinful model leads to two distinct phases, depending on the various Luttinger parameters and initial amplitudes of the nonquadratic terms. (1) Tunneling is the dominant interaction: Tunneling is more relevant than the $2k_F$ backscattering term for $K_\rho > \frac{1}{3} - \frac{1}{36}U$, and tends to open a gap $\Delta_t \propto t_\perp^{1/[3/2 - 1/4(K_{\rho+} + 1/K_{\rho-})]}$ for fluctuations of the density in the total sectors and of the phase in the relative sectors. (2) Backscattering is dominant: In this regime, the $2k_F$ backscattering term opens a gap $\Delta_{BS} \propto |V_{BS}|^{1/(1 - K_{\rho+})}$ for relative spin fluctuations, which suppresses tunneling up to Δ_{BS} . This phase is characterized by a spin gap and quasi-long-ranged charge density wave correlations at wave vector $2k_F$. We denote it as a Wigner crystal.

The zero temperature tunneling current-voltage characteristics of the two phases are shown in Figs. 4(a) and 4(b). When the voltage is greater than the gap (either Δ_t or Δ_{BS}), a linear response calculation may again be used. The derivation is identical to that of the spinless case, only now $A(x, t) = \sum_\sigma c_{1\sigma}^\dagger(x, t) c_{-1\sigma}(x, t)$, with σ signifying spin. The resulting current follows a power-law dependence, $I_t(V) \propto V^{\frac{1}{2}(K_{\rho+} + K_{\rho-}^{-1}) - 1}$. The exponent can have either sign, depending on the strength of the interwire versus intrawire interactions. As in the spinless case, a negative exponent is again a signature of interwire exciton quasicondensation. In the backscattering dominated phase, the current goes abruptly

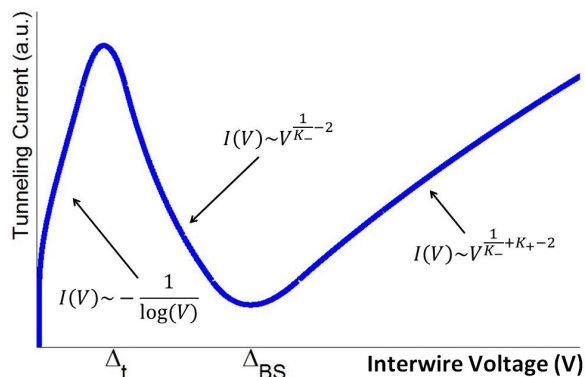


FIG. 3. (Color online) Current-voltage characteristics for spinless fermions, in the case of relevant interwire tunneling. The tunneling current obeys the singular relationship $I(V) \propto -1/\log(V)$ for voltages lower than the tunneling gap, while at higher voltages it reverts to a power law in the voltage, with the exponent increasing as the difference is amplified. For a large set of values of K_+ , K_- quite accessible experimentally, the exponent may be negative in some voltage regime, as shown in this figure, corresponding to a negative differential conductance. This is because in the regime $\Delta_t \ll V \ll \Delta_{BS}$, the total sector is locked by the backscattering gap, and K_+ is reduced while K_- is increased by interwire forward scattering.

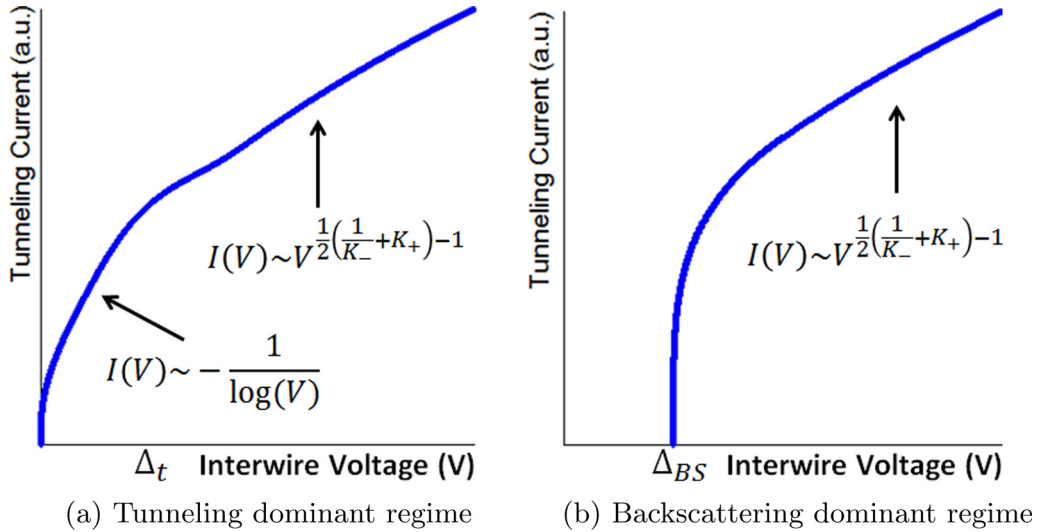


FIG. 4. (Color online) I - V curve for spinful electrons in the regimes where tunneling or backscattering is dominant. In the tunneling dominant regime, the low voltage current obeys the singular relationship $I(V) \propto \frac{-1}{\log(V)}$, as the current dissipates through the macroscopic tunneling mechanism described in Sec. II. At high voltages, the current is a power law in the voltage, $I(V) \propto V^{\frac{1}{2}(K_{\rho+} + K_{\rho-}^{-1}) - 1}$. The presence of noninteracting spin sectors ($K_{\sigma} = 1$) and interwire forward scattering U may decrease the exponent to negative values, resulting in a negative differential conductance, which is a mark of an exciton quasicondensate. In the regime where backscattering is dominant, the interaction opens a gap Δ_{BS} for relative spin fluctuations which suppresses tunneling up to that scale. At $V \gg \Delta_{BS}$, the current obeys the power law $I(V) \propto V^{\frac{1}{2}(K_{\rho+} + K_{\rho-}^{-1}) - 1}$.

to zero when the voltage is below Δ_{BS} . In contrast, in the tunneling dominated phase, at small voltages the current has a logarithmic dependence on voltage, $I_t(V) \propto -1/\log(V/\Delta_t)$, as in the spinless case. This is again the result of an instantonic process, as in the spinless case. The tunneling conductivity $\sigma = \lim_{V \rightarrow 0} \frac{dI_t}{dV}$ diverges at low voltages.

If the intrawire interactions are strong, additional backscattering terms arise. In this case, the density correlations in each wire become strongly peaked at a wave vector of $4k_F$, and the amplitude of the $4k_F$ ultimately becomes stronger than the $2k_F$ component [20]. The coupling of the $4k_F$ Fourier components of the density in the two wires leads to an additional backscattering term of the form

$$H_{BS,4k_F} = -|V_{BS,4k_F}| \int dx \cos(4\phi_{\rho+}). \quad (16)$$

This term, while less relevant than H_{BS} , has a large amplitude in the strongly interacting limit. In this case, a gap in the $\rho+$ sector can open at an energy larger than Δ_t, Δ_{BS} . In the tunneling dominated phase, this will result in an I - V curve more similar to the one shown in Fig. 3, with two characteristic energy scales: $\Delta_{BS,4k_F}$ at which the $\rho+$ sector becomes gapped, and Δ_t . We will discuss the effects of the $4k_F$ backscattering term in more detail in a future publication.

Before concluding, let us mention the signatures of the two phases in the drag resistance between the two wires. Although $2k_F$ backscattering suppresses excitonic correlations, which are proportional to

$$\begin{aligned} & \sum_{\sigma\sigma'} \langle c_{1\sigma R}^\dagger(x) c_{-1\sigma L}(x) c_{-1\sigma' L}^\dagger(0) c_{1\sigma' R}(0) \rangle \\ & \propto x^{1/2(K_{\rho+} + 1/K_{\rho-} + K_{\sigma+} - 1/K_{\sigma-})} \end{aligned} \quad (17)$$

due to the locking of the relative spin density, the drag resistance diverges in the backscattering dominated phase at low temperatures [9,10,21–26], since the $\phi_{\rho+}$ is locked. In this respect, a divergent drag resistance does not signify enhanced excitonic correlations in our system. The tunneling dominated phase is insulating at temperatures below Δ_t , so measuring drag resistance is impossible unless a large bias voltage $V > \Delta_t$ is applied to one of the wires.

IV. CARBON NANOTUBES

An obvious experimental realization of the system considered in this work is a double carbon nanotube setup. The two metallic nanotubes can be brought closely together and gated independently. The linearity of the spectrum, for both armchair and zigzag nanotubes, insures particle-hole symmetry, which favors exciton formation, as such a symmetry results in a nested Fermi surface towards the creation of particle-hole excitations with zero momentum. The gapless spectrum allows the use of arbitrarily small voltages for doping, negating a possible effect of gating on the band structure. Finally, carbon nanotubes may be fabricated with an exceptional purity, rendering our neglect of disorder in the previous analysis tenable.

In addition to spin, metallic carbon nanotubes have a valley degree of freedom [27]. Applying a magnetic field along the axis of the nanotubes lifts the valley degeneracy, as well as the spin degeneracy; one can design systems in which either the valley, the spin, or both are quenched (i.e., only a electrons of a single spin or valley flavor cross the Fermi energy) [28]. In these cases, the analysis of the previous two sections goes through without modification. Here, we comment briefly on the valley degenerate case (no magnetic field).

Denoting the valley label by $\nu = \pm 1$, we define the boson fields $\phi_{\mu\pm} = \frac{1}{\sqrt{2}}(\phi_{\mu\nu\nu=1} + \phi_{\mu\nu\nu=-1})$ and $\phi_{\mu\pm r} =$

$\frac{1}{\sqrt{2}}(\phi_{\mu\pm v=1} - \phi_{\mu\pm v=-1})$, with $\mu = \rho, \sigma$ as before. Intervalley scattering is very much suppressed in carbon nanotubes [29], and therefore we assume that $K_{\rho+r} = K_{\sigma+t} = K_{\sigma+r} = K_{\rho-r} = K_{\sigma-t} = K_{\sigma-r} = 1$. The interaction strength is encoded in the Luttinger parameters $K_{\rho\pm t} = \frac{K_{\rho t}}{\sqrt{1\pm U K_{\rho t}}}$, where $K_{\rho t}$ is the Luttinger parameter for the total charge

$$H_{\text{BS}} = - |V_{\text{BS}}| \{ \cos(\sqrt{2}\phi_{+\rho t}) \cos(\sqrt{2}\phi_{+\rho r}) [\cos(\sqrt{2}\phi_{+\sigma t}) \cos(\sqrt{2}\phi_{+\sigma r}) + \cos(\sqrt{2}\phi_{-\sigma t}) \cos(\sqrt{2}\phi_{-\sigma r})] \\ + \cos(\sqrt{2}\phi_{+\rho t}) \cos(\sqrt{2}\phi_{-\rho r}) [\cos(\sqrt{2}\phi_{+\sigma t}) \cos(\sqrt{2}\phi_{-\sigma r}) + \cos(\sqrt{2}\phi_{-\sigma t}) \cos(\sqrt{2}\phi_{+\sigma r})] \}, \quad (18)$$

while the interwire tunneling term has the form

$$H_{\text{tun}} = -\tilde{t} \int dx \sum_{\eta_1=\pm 1} \sum_{\eta_2=\pm 1} \exp \left(\frac{i}{\sqrt{2}} [\phi_{\rho+t} + \eta_1 \phi_{\rho+r} - \theta_{\rho-t} - \eta_1 \theta_{\rho-r} + \eta_2 (\phi_{\sigma+t} + \eta_1 \phi_{\sigma+r} - \theta_{\sigma-t} - \eta_1 \theta_{\sigma-r})] + i \frac{\pi}{2} \right) + \text{H.c.} \quad (19)$$

The lowest-order β functions of the two terms are given by

$$\frac{dV_{\text{BS}}}{ds} = \frac{1}{2} [1 - K_{\rho+t}] V_{\text{BS}}, \quad (20)$$

$$\frac{dt_{\perp}}{ds} = \left[\frac{5}{4} - \frac{1}{8} \left(K_{\rho+t} + \frac{1}{K_{\rho-t}} \right) \right] t_{\perp}.$$

The addition of internal degrees of freedom, such as valley, enhances the possibility for exciton condensation, in comparison to the results of spinful, valleyless electrons; the phase where the tunneling conductivity is the most divergent corresponds to intrawire Luttinger parameters obeying $K_{\rho} > 0.15 - 0.01U$ for small U . This regime is accessible in experiments; the experimental estimates for the Luttinger parameter of single walled nanotubes [13,30] are in the range $K_{\rho} \sim 0.2-0.3$, resulting in a more divergent tunneling operator, and thus the tunneling dominated phase may be reached. In this phase, the low voltage tunneling current will obey the familiar $I_t(V) \propto \frac{-1}{\log(V)}$ law, while for voltages much higher than any emergent gap in the system, the current will again be a power law in the voltage, with the exponent modified by the additional noninteracting sectors, resulting in $I_t(V) \propto V^{\frac{1}{4}(K_{\rho+t} + K_{\rho-t}) - \frac{1}{2}}$.

V. CONCLUSION

In conclusion, we consider a system of oppositely doped wires in the limit of strong forward scattering and weak interwire backscattering and tunneling. For strong enough interwire interactions, the system is susceptible to excitonic quasi-long-range order. We further discuss the tunneling current-voltage characteristics, and show that there are three different regimes, depending on the relative relevance and magnitude of the tunneling process and the two types of interwire backscattering. When the tunneling process is dominant, a signature of strong excitonic correlations may appear in the form of a negative differential resistance, making tunneling a probe of interwire phase coherence. On the other hand, we argue that the drag resistance will diverge both in the excitonic regime and in the Wigner crystal, where the phases of the two wires are independent. Lastly, we examine carbon nanotubes,

for a single wire, and U the interwire forward scattering potential.

As in the spinful valleyless case, the interwire backscattering term (16) tends to lock both total (+) and relative (-) modes, and thus competes with the tunneling term (17). The backscattering term is written as

and note that they are exceptionally suited for the detection of excitons.

ACKNOWLEDGMENTS

We thank S. Ilani and B. Rosenow for useful discussions. This work was supported by the Israel Science Foundation, the Minerva fund, and a Marie Curie Career Integration Grant (CIG).

APPENDIX A: SIGN ISSUES

In bosonization theory, electrons of the same species obey fermion statistics due to the commutation relations of the bosons ϕ and θ , while the anticommutation of different species must be put in by hand [11]. One way to achieve this is to impose the following relationship between θ 's of different electrons [31],

$$[\theta_i(x), \theta_j(x')] = i\pi \epsilon_{ij}, \quad (A1)$$

where ϵ_{ij} is the antisymmetric tensor.

1. Interwire backscattering

One consequence of the anticommutation of fermions is the sign of the backscattering term. Consider the operator

$$c_{1R}^{\dagger}(x) c_{1L}(x) \\ \propto \exp [i(\phi_1(x) - \theta_1(x))] \exp [-i(-\phi_1(x) - \theta_1(x))] \\ = \exp [2i\phi_1(x)] e^{\frac{i}{2}[\phi_1(x) - \theta_1(x), -\phi_1(x) - \theta_1(x)]}, \quad (A2)$$

where the second term on the last line is a consequence of the Baker-Hausdorff formula. The commutator can be evaluated easily using the convention

$$[\phi(x), \theta(x')] = i\pi \Theta(x - x') \quad (A3)$$

along with the point-splitting technique [11]; it results in

$$c_{1R}^{\dagger}(x) c_{1L}(x) \propto -i \exp [2i\phi_1(x)]. \quad (A4)$$

Therefore,

$$\begin{aligned} c_{1R}^\dagger(x)c_{1L}(x)c_{-1R}^\dagger(x)c_{-1L}(x) \\ \propto i \exp[2i\phi_1(x)] i \exp[2i\phi_{-1}(x)] \\ = -\exp[2\sqrt{2}i\phi_+(x)], \end{aligned} \quad (\text{A5})$$

incurring a minus sign that is absent for wires doped equally with the same kind of charge carrier, where backscattering is of the form $c_{1R}^\dagger c_{1L} c_{-1L}^\dagger c_{-1R}$.

2. Tunneling

The form of the tunneling term is also affected by the fermionic phase,

$$\begin{aligned} c_{1R}^\dagger c_{-1L} \propto e^{i(\phi_1+\phi_{-1}-\theta_1+\theta_{-1})} e^{\frac{1}{2}[\theta_1, \theta_{-1}]} \\ = i e^{i(\phi_1+\phi_{-1}-\theta_1+\theta_{-1})}, \end{aligned} \quad (\text{A6})$$

with equivalent phases for the other three components of the tunneling interaction, which result in the form given by Eq. (4). The addition of spin generates terms of the form

$$c_{1R\uparrow}^\dagger c_{-1L\downarrow} = e^{i(\phi_{\rho+}-\theta_{\rho-}+\phi_{\sigma+}-\theta_{\sigma-})} e^{\frac{1}{4}([\theta_{1\rho}, \theta_{-1\rho}] + [\theta_{1\sigma}, \theta_{-1\sigma}])}, \quad (\text{A7})$$

resulting again in a factor i , and leading to Eq. (13).

APPENDIX B: INSTANTON CALCULATION

The real time action governing the evolution of the relative phase is given by

$$\begin{aligned} S = \frac{u-K_-}{2\pi} \int dx dt \left(\frac{1}{u_-^2} (\partial_t \theta_-)^2 - (\partial_x \theta_-)^2 \right) \\ + \int dx dt \left[J \sin(\sqrt{2}\theta_-) + \frac{\sqrt{2}}{e} \mathcal{J} \theta_- \right], \end{aligned} \quad (\text{B1})$$

where, as in Sec. II, $J = t_\perp (\cos(\sqrt{2}\phi_+))$ and \mathcal{J} is the current density driven between the wires, which breaks the symmetry between the minima of the sine-Gordon potential.

The decay rate of the metastable state $\sqrt{2}\theta_0 = \frac{\pi}{2}$ can be calculated from the Green's function $G(T) = \langle \theta_0 | e^{iHT} | \theta_0 \rangle$, which, after analytic continuation, becomes

$$G(\tau) = \langle \theta_0 | e^{H\tau} | \theta_0 \rangle = \int \mathcal{D}[\theta(\tau')] e^{-S_E[\theta(\tau)]}, \quad (\text{B2})$$

where the Euclidean action S_E is given by

$$\begin{aligned} S = \frac{u-K_-}{2\pi} \int dx d\tau \left(\frac{1}{u_-^2} (\partial_\tau \theta_-)^2 + (\partial_x \theta_-)^2 \right) \\ - \int dx d\tau \left[J \sin(\sqrt{2}\theta_-) + \frac{\sqrt{2}}{e} \mathcal{J} \theta_- \right]. \end{aligned} \quad (\text{B3})$$

We evaluate this path integral by a saddle point approximation, corresponding to field configurations $\{\theta_-(x, \tau)\}$ which satisfy the Euler-Lagrange equations

$$\partial_r^2 \theta + \frac{1}{r} \partial_r \theta = -\frac{\sqrt{2}\pi}{uK} \left[J \cos(\sqrt{2}\theta) + \frac{\mathcal{J}}{e} \theta \right], \quad (\text{B4})$$

where we have defined $r = \sqrt{x^2 + u^2\tau^2}$.

For $\mathcal{J} \ll eJ$, meaning that the potential minimum asymmetry imposed by the current \mathcal{J} is small, it is possible to use the thin wall approximation [32]; in this case, it is assumed that the configurations which minimize the action are described by a domain wall of thickness Δr which is positioned at $r_0 \gg \Delta r$, which separates regions of homogenous configurations of θ — $\theta(r < r_0) = \frac{\pi}{2}$, $\theta(r > r_0) = \frac{5\pi}{2}$. In this case, the second term on the left hand side of Eq. (B4) is much smaller than the first, and the Euler-Lagrange equations are

$$\partial_r^2 \theta \approx -\frac{2\sqrt{2}\pi}{uK} \left[J \cos(\sqrt{2}\theta) + \frac{\mathcal{J}}{e} \theta \right]. \quad (\text{B5})$$

The configurations satisfying this equation are known as instantons, and they describe kinks in the otherwise constant configuration of the θ field. Their action consists of two parts: (1) The action cost of the kink, which scales as $2\pi r_0$, as the kink occurs only along the domain wall. It may be calculated for $\mathcal{J} = 0$ with the assistance of the Euler-Lagrange equation, and results in

$$S_0 \approx 2.5 \sqrt{\frac{uK}{2\pi}} J. \quad (\text{B6})$$

(2) The action cost of the field being in a metastable minimum, which has an energy larger by $\Delta\epsilon = 2\pi \frac{\mathcal{J}}{e}$. This contribution scales as πr_0^2 , which is the size of the domain in which the field is in the higher energy state.

Therefore, the total action which corresponds to a propagating domain wall in the presence of a nonvanishing current is

$$S = 2\pi r_0 S_0 - \pi^2 r_0^2 \frac{\mathcal{J}}{e}. \quad (\text{B7})$$

The minimum of this action occurs for $r_0 = S_0/(\pi \frac{\mathcal{J}}{e})$, and corresponds to the total action

$$S = \frac{S_0^2 e}{\mathcal{J}}. \quad (\text{B8})$$

However, this action is not the only contribution to the path integral that can be obtained from the saddle point approximation. Since the kink of the instanton is localized in time, it is feasible to assume that any number of instantons, separated such that they can be considered as noninteracting in the sense that the total action is simply the addition of n single instanton actions S_{inst} , is also a saddle point configuration. The path integral that is obtained for the Green's function (A2) is therefore

$$\begin{aligned} G(\tau) &\approx \sum_n C^n \int_0^\tau d\tau_1 \cdots \int_0^{\tau_{n-1}} d\tau_n e^{-nS} \\ &= \sum_n \frac{1}{n!} (C\tau e^{-S})^n \\ &= e^{C\tau e^{-S}}, \end{aligned} \quad (\text{B9})$$

where the n -fold integration occurs due to space-time translation invariance; the value of r at which the kink occurs can vary between 0 and r for $r \rightarrow \infty$. C is a dimensionful constant which arises from the Gaussian fluctuations around the minima of action, and from normalization factors.

Applying the analytic continuation, and relying on the fact that K must be pure imaginary [32],

$$G(t) \propto e^{-t|C|e^{-S}}, \quad (\text{B10})$$

and it follows that the tunneling rate from the metastable minimum is

$$\Gamma = |C|e^{-S} \propto e^{-\frac{S^2 c}{\mathcal{J}}}. \quad (\text{B11})$$

-
- [1] J. P. Eisenstein and A. H. MacDonald, *Nature (London)* **432**, 691 (2004).
- [2] J. A. Seamons, D. R. Tibbetts, J. L. Reno, and M. P. Lilly, *Appl. Phys. Lett.* **90**, 052103 (2007).
- [3] D. Nandi, A. D. K. Finck, J. P. Eisenstein, L. N. Pfeiffer, and K. W. West, *Nature (London)* **488**, 481 (2012).
- [4] K. Das Gupta, A. F. Croxall, J. Waldie, C. A. Nicoll, H. E. Beere, I. Farrer, D. A. Ritchie, and M. Pepper, *Adv. Condens. Matter Phys.* **2011**, 727958 (2011).
- [5] D. Laroche, G. Gervais, M. P. Lilly, and J. L. Reno, *Science* **343**, 631 (2014).
- [6] I. B. Spielman, J. P. Eisenstein, L. N. Pfeiffer, and K. W. West, *Phys. Rev. Lett.* **84**, 5808 (2000).
- [7] This is a one-dimensional analog of the setup proposed by H. Min, R. Bistritzer, J.-J. Su, and A. H. MacDonald, *Phys. Rev. B* **78**, 121401 (2008).
- [8] D. G. Shelton and A. M. Tsvelik, *Phys. Rev. B* **53**, 14036 (1996).
- [9] R. Klesse and A. Stern, *Phys. Rev. B* **62**, 16912 (2000).
- [10] M. Pustilnik, E. G. Mishchenko, L. I. Glazman, and A. V. Andreev, *Phys. Rev. Lett.* **91**, 126805 (2003).
- [11] T. Giamarchi, *Quantum Physics in One Dimension* (Clarendon, Oxford, UK, 2003).
- [12] D. N. Aristov, A. P. Dmitriev, I. V. Gornyi, V. Y. Kachorovskii, D. G. Polyakov, and P. Wölfle, *Phys. Rev. Lett.* **105**, 266404 (2010).
- [13] M. Bockrath, D. H. Cobden, J. Lu, A. G. Rinzler, R. E. Smalley, L. Balents, and P. L. McEuen, *Nature (London)* **397**, 598 (1999).
- [14] O. M. Auslaender, A. Yacoby, R. de Picciotto, K. W. Baldwin, L. N. Pfeiffer, and K. W. West, *Science* **295**, 825 (2002).
- [15] Y. Jompol, C. J. B. Ford, J. P. Griffiths, I. Farrer, G. A. C. Jones, D. Anderson, D. A. Ritchie, T. W. Silk, and A. J. Schofield, *Science* **325**, 597 (2009).
- [16] T. Hyart and B. Rosenow, *Phys. Rev. B* **83**, 155315 (2011).
- [17] G. D. Mahan, *Many-Particle Physics* (Springer, Berlin, 2000).
- [18] P. Johansson and J. M. Kinaret, *Phys. Rev. B* **50**, 4671 (1994).
- [19] M. Tinkham, *Introduction to Superconductivity* (Dover, New York, 2004).
- [20] S. R. White, I. Affleck, and D. J. Scalapino, *Phys. Rev. B* **65**, 165122 (2002).
- [21] R. G. Pereira and E. Sela, *Phys. Rev. B* **82**, 115324 (2010).
- [22] S. Teber, *Phys. Rev. B* **76**, 045309 (2007).
- [23] K. Flensberg, *Phys. Rev. Lett.* **81**, 184 (1998).
- [24] Y. V. Nazarov and D. V. Averin, *Phys. Rev. Lett.* **81**, 653 (1998).
- [25] V. V. Ponomarenko and D. V. Averin, *Phys. Rev. Lett.* **85**, 4928 (2000).
- [26] G. A. Fiete, K. Le Hur, and L. Balents, *Phys. Rev. B* **73**, 165104 (2006).
- [27] S. Dresselhaus, G. Dresselhaus, and P. Avouris, *Carbon Nanotubes: Synthesis, Structure, Properties, and Applications* (Springer, Berlin, 2001).
- [28] F. Kuemmeth, S. Ilani, D. C. Ralph, and P. L. McEuen, *Nature (London)* **452**, 448 (2008).
- [29] C. Kane, L. Balents, and M. P. A. Fisher, *Phys. Rev. Lett.* **79**, 5086 (1997).
- [30] Z. Yao, H. W. C. Postma, L. Balents, and C. Dekker, *Nature (London)* **402**, 273 (1999).
- [31] J. von Delft and H. Schoeller, *Ann. Phys.* **7**, 225 (1998).
- [32] A. Altland and B. Simons, *Condensed Matter Field Theory* (Cambridge University Press, Cambridge, UK, 2010).